Contents lists available at ScienceDirect

Translational Oncology

Evaluation of ^{99m}Tc-CN5DG as a broad-spectrum SPECT probe for tumor imaging

Xuran Zhang, Qing Ruan, Yuhao Jiang, Qianqian Gan, Junbo Zhang*

Key Laboratory of Radiopharmaceuticals of Ministry of Education, College of Chemistry, Beijing Normal University, Beijing 100875, PR China

ARTICLE INFO

ABSTRACT

Previously, we reported a $[^{99m}Tc(|)]^+$ labeled D-glucoamine derivative (^{99m}Tc-CN5DG) and evaluated it as a tumor imaging agent in mice bearing A549 tumor xenografts. In this paper, ^{99m}Tc-CN5DG was further studied in U87 MG (human glioma cells), HCT-116 (human colon cancer cells), PANC-1 (human pancreatic cancer cells) and TE-1 (human esophageal cancer cells) tumor xenografts models to verify its potential application for imaging of different kinds of tumors. The biodistribution data showed that ^{99m}Tc-CN5DG had a similar biodistribution pattern in four tumor models at 2 h post-injection with high accumulation in tumors and kidneys. The tumor/muscle ratios (from 4.08 ± 0.42 to 9.63 ± 3.53) and tumor/blood ratios (from 17.18 ± 7.40 to 53.17 ± 16.16) of ^{99m}Tc-CN5DG in four tumor models were high. All four kinds of tumors could be clearly seen on their corresponding SPECT/CT images. Pharmacokinetic study in healthy CD-1 mice demonstrated that ^{99m}Tc-CN5DG cleared fast from blood (2 min, 12.97 ± 0.88%ID/g; 60 min, 0.33 ± 0.06%ID/g) and the blood distribution, elimination half-life was 5.81 min and 21.16 min, respectively. No abnormality was observed through the abnormal toxicity study. All of the above results demonstrated that ^{99m}Tc-CN5DG could be a broad-spectrum SPECT probe for tumor imaging and its further clinical application is warranted.

Introduction

Nuclear medicine molecular imaging plays an increasingly important role in disease diagnosis and treatment over the past few decades [1, 2]. Positron Emission Tomography (PET) and Single Photon Emission Tomography (SPECT) are the two main imaging modalities that are used annually in the whole world. As we know, tumor cells need to consume more glucose to meet their enhanced metabolic rate. 2-[^{18}F]fluoro-2-deoxy-D-glucose ([^{18}F]FDG) is the most used PET radiopharmaceutical for various cancer diagnosis (such as lung cancer, breast cancer, lymphoma, esophageal cancer, pancreatic cancer) and staging due to its similar chemical structure to glucose [3-7]. However, in most developing countries, the use of [^{18}F]FDG has limitation due to the need of a cyclotron for producing ^{18}F isotope and high cost. In addition, another drawback of [^{18}F]FDG is the fact that also non-FDG-avid tumors exist.

^{99m}Tc is the most used nuclide for SPECT because of its inexpensive cost and availability from the ^{99}Mo/^{99m}Tc generator. Besides, the overall number of SPECT scanners is far more than PET scanners in the whole world. Therefore, the development of ^{99m}Tc labeled glucose derivatives as broad-spectrum SPECT probes for tumor imaging is necessary but remains challenging. Although ^{99m}Tc labeled glucose derivatives for tumor imaging has been studied for about three decades, no one has been approved for routine use for tumor diagnosis in clinic [8-16].

Over the past ten years, we have been working on this field in order to develop a ^{99m}Tc labeled glucose derivative with high tumor uptake and low background uptake [17-23]. Fortunately, a D-glucoamine derivative with an isonitrile group (CN5DG) was synthesized and radiolabeled with ^{99m}Tc(|) to produce ^{99m}Tc-CN5DG (Fig. 1). Preliminary studies in A549 tumor xenografts demonstrated that ^{99m}Tc-CN5DG would be a powerful tool as a SPECT probe for tumor detection [24]. In order to verify the effectiveness of ^{99m}Tc-CN5DG for detecting other kinds of tumor models, we conducted the evaluation of ^{99m}Tc-CN5DG on four different human cell lines (U87 MG, human glioma cells; HCT-116, human colon cancer cells; PANC-1, human pancreatic cancer cells; TE-1, human esophageal cancer cells) to explore its feasibility as a broad-spectrum SPECT probe for tumor imaging. Moreover, its stability *in vivo* and pharmacokinetic properties are also studied.

Materials and methods

Materials and equipments

CN5DG kit which contains 0.5 mg CN5DG, 2.6 mg sodium citrate, 1 mg L-cysteine, 100 μg SnCl$_2$•2H$_2$O and 20 mg mannitol was obtained from Beijing Shihong Pharmaceutical Center, Beijing, China. Radiochemical purity was analyzed by a HPLC system equipped with a Waters
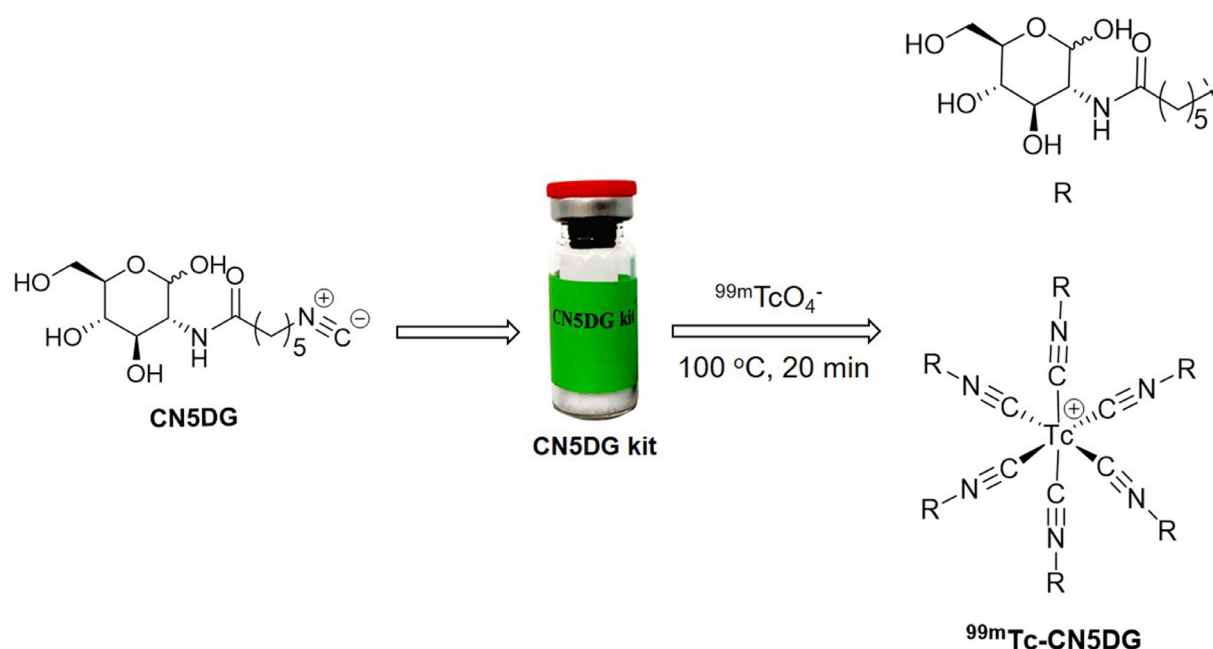
Fig. 1. Preparation of ^{99m}Tc-CN5DG and the chemical structure of CN5DG and ^{99m}Tc-CN5DG.

2489 UV and a Gabi raytest radioactivity detector using an analytical column (18C, Kromasil, 100–5 μm, 250 × 4.6 mm). The HPLC gradient elution method was: (A, purified water; B, acetonitrile). 0–2 min, 10% B; 2–17 min, 10%–90% B; 17–20 min, 90% B; 20–25 min, 90%–10% B; 25–30 min, 10%B. ^{99m}TcO$_4^-$ was eluted from a ^{99}Mo/^{99m}Tc generator (Atomic High Technology Co., Ltd, Beijing, China). Radioactivity was recorded by a Gamma Counter (WIZARD$^{2®}$2480 Perkin-Elmer system). SPECT/CT images were acquired on a small animal SPECT/CT scanner (Triumph SPECT/CT, console-gr157, USA).

Animals and tumor models

Balb/c nude mice (14–16 g) and CD-1 mice were purchased from Beijing Vital River Laboratory Animal Technology Co., Ltd (Beijing, China) and animal studies were conducted in compliance with the Regulations on Laboratory Animals of Beijing Municipality and the guidelines of the Ethics Committee of Beijing Normal University. HCT116, PANC-1 and TE-1 cells were purchased from Cell Bank of Chinese Academy of Sciences (Shanghai, China). U87 MG cells were obtained from Key Laboratory of Radiopharmaceuticals of Ministry of Education, Beijing Normal University. U87 MG, HCT116, PANC-1 and TE-1 cells were cultured in MEM, IMDM, DMEM and RPMI 1640 (ATCC modified) medium containing 10% FBS and 1% penicillin-streptomycin, respectively. Tumor xenografts bearing mice models were developed by injecting tumor cells (3~5 × 10^6 cells) into the right forelimb of balb/c nude mice subcutaneously. Biodistribution and SPECT/CT imaging studies were carried out when the tumors reached 0.3–0.6 cm in diameter after 7–14 days post-inoculation.

Biodistribution studies

^{99m}Tc-CN5DG was successfully prepared using a CN5DG kit according to previous published literature [24]. ^{99m}Tc-CN5DG (0.1 mL, 74 kBq) was injected into nude mice bearing different tumor xenografts (U87 MG, HCT116, PANC-1, TE-1, n = 3) via the tail vein. The animals were sacrificed at 2 h post-injection. The interested tissues or organs (such as heart, liver, tumor, lung, kidney) were removed, weighted and their radioactivity were recorded by a gamma counter. The uptake values were calculated as the percentage of the injected dose per gram

(%ID/g). The uptake results were presented as average ± SD (standard derivation) of 3 animals.

SPECT/CT imaging studies

55.5–74 MBq of ^{99m}Tc-CN5DG was injected into mice (n = 3 for each tumor model) and the mice were scanned at 2 h post-injection using a small animal SPECT/CT scanner (3 D whole-body scan, MMP 919 collimator). SPECT/CT images were reconstructed by HiSPECT software and analyzed by a Vivoquant 2.5 software.

Dynamic uptake SPECT studies of ^{99m}Tc-CN5DG was performed on nude mice bearing U87 MG tumor xenografts. 18.5 MBq of ^{99m}Tc-CN5DG was injected into the mice and the SPECT data were acquired continuously from 5 to 60 min after injection (half-body scan, MMP 930 collimator). The dynamic SPECT images were generated from every 5 min's SPECT data. The Regions of Interest (ROIs) from tumor tissues and the ROIs from muscle were drawn on SPECT images.

Metabolic studies *in vivo*

^{99m}Tc-CN5DG (0.1–0.2 mL, 2 mCi) was injected into A549 tumor bearing nude mice (n = 3) via the tail vein. The mice were sacrificed at 30 min post-injection, then blood and tumor were collected. The blood was centrifuged at 10,000 rpm for 5 min. 300 μL of the supernatant was mixed with 600 μL of acetonitrile. The precipitated protein was removed by centrifugation and the supernatant was collected, concentrated and then analyzed by HPLC. For metabolic stability in tumor, the separated tumors were homogenized by a tissue-tearor (DREMEL, Model 3000) and the tumor homogenate was passed through a 0.22 μm membrane. To the filtrate, 600 μL of acetonitrile was added and the precipitated protein was removed by centrifugation, then the supernatant was collected, concentrated and analyzed by HPLC.

Pharmacokinetic characteristics

36 normal female CD-1 mice (18–22 g) were divided into 6 groups (6 mice for one group, 3 female mice and 3 male mice). 370 kBq of ^{99m}Tc-CN5DG was injected into the mice via the tail vein. The mice were killed at 2 min, 10 min, 30 min, 60 min, 120 min and 240 min post-injection
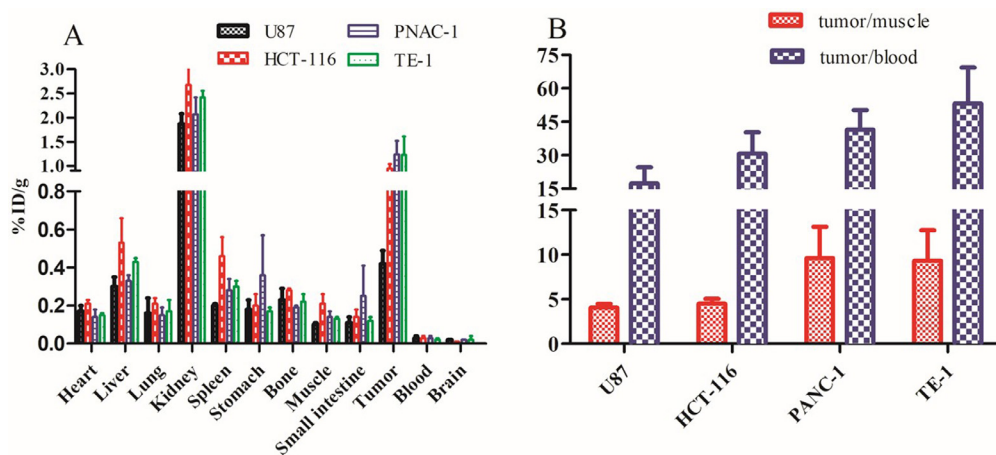
Fig. 2. (A) Biodistribution data of ^{99m}Tc-CN5DG in nude mice bearing U87 MG, HCT-116, PANC-1 and TE-1 tumors at 2 h post-injection. (B) Comparison of the tumor/muscle and tumor/blood ratios in four tumor models.

[25]. The blood samples were collected, weighted and the radioactivity were recorded by a gamma counter. The blood uptake value was presented as%ID/g ± SD of 6 animals. The blood uptake-time curves were generated and analyzed by DAS 3.2.8 software.

Abnormal toxicity studies

For novel radiopharmaceuticals, the abnormal toxicity was within consideration. Thus, we carried out the toxicity of the solution of ^{99m}Tc-CN5DG according to the regulation of pharmacopoeia of People's Republic of China (2015 Edition). The total volume of the reaction mixture was adjusted to 5 mL. Then, 0.5 mL of this solution were injected to healthy CD-1 mice ($n = 5$, 18–20 g) via the tail vein. The toxicity of the solution was determined by observing the death and survival of mice in the next 48 h.

Statistical analysis

The biodistribution data were calculated and analyzed with Microsoft Excel 2016 and Prism 5.01. All data were presented as average ± SD. To compare differences between two data, the one tail-paired student t-test was used. $P < 0.05$ indicated a statistically significant difference.

Results

Biodistribution studies

The biodistribution patterns (Fig. 2) were similar in all four kinds of tumor models with high accumulation in kidneys and tumors. Among the four tumor models, the uptake of ^{99m}Tc-CN5DG in HCT-116, PANC-1 and TE-1 tumors (from 0.95 ± 0.09%ID/g to 1.24 ± 0.28%ID/g) were higher than that in U87 MG tumors (0.42 ± 0.07%ID/g). The tumor/muscle ratios in U87 MG, HCT-116, PANC-1 and TE-1 were 4.02 ± 0.42, 4.53 ± 0.54, 9.63 ± 3.53 and 9.35 ± 3.38, respectively. The tumor/blood ratios in PANC-1 (41.41 ± 8.75) and TE-1 (53.17 ± 16.16) tumor models were significantly higher than that in U87 MG (17.18 ± 7.40) and HCT-116 (30.59 ± 9.62) tumor models. The high tumor/blood ratios in all four tumor models indicated that ^{99m}Tc-CN5DG has low blood uptake. Taken together, these results demonstrated that ^{99m}Tc-CN5DG had a significant uptake in a variety of tumors and would be more suitable for the detection of PANC-1 and TE-1 tumors.

SPECT/CT studies

SPECT/CT three-dimensional whole body images were acquired at 2 h after the injection of ^{99m}Tc-CN5DG (74 MBq) via the tail vein ($n = 3$). From the SPECT/CT images (Fig. 3), tumors could be clearly seen in

all four tumor models. The ROI ratios of the tumor sites *versus* corresponding non-tumor sites for U87 MG, HCT-116, PANC-1 and TE-1 were 3.09 ± 0.19, 4.73 ± 0.15, 5.51 ± 0.79 and 6.01 ± 1.37, respectively. Moreover, kidney and bladder could also clearly seen from the SPECT/CT images, suggesting its clearance way was through the urinary system. These results were in consistence with the biodistribution data and verified that ^{99m}Tc-CN5DG holds potential for the diagnosis of glioma, colon cancer, pancreatic cancer and esophageal cancer.

Dynamic SPECT images (5–60 min) in nude mice bearing U87 MG tumor xenografts were shown in Fig. 4. From the SPECT images (Fig. 4A), U87 MG tumors could be clearly seen from 5 min to 60 min post-injection. The tumor uptake value reached the highest before 30 min after injection and cleared slowly afterwards. The tumor/muscle ratios (ROI ratios) drawn from the SPECT images were shown in Fig. 4B. The values increased from 1.79 (5–10 min) to 2.89 (55–60 min) and reached a plateau at about 50 min post-injection.

Metabolic studies in vivo

To investigate the metabolic stability of ^{99m}Tc-CN5DG in blood and tumor *in vivo*, A549 tumor xenografts bearing nude mice were used. As shown in Fig. 5a, the retention time of co-injection (control and tumor) was 13.19 min, indicating that ^{99m}Tc-CN5DG kept intact in tumor. As shown in Fig. 5b, the retention time (13.57 min) of ^{99m}Tc-CN5DG in blood at 30 min after intravenous injection was consistent with the control (13.85 min), suggesting its stability in blood *in vivo*. Combined with our previous studies, we concluded that ^{99m}Tc-CN5DG was transported into tumor cells through glucose transporters and was not further metabolized in tumors [24].

Pharmacokinetic characteristics

The pharmacokinetic parameters were calculated by the statistical moment method of the two-compartment model using DAS 3.2.8 software. Time-activity curve of blood of ^{99m}Tc-CN5DG in healthy CD-1 mice was shown in Fig. 6. The blood uptake of ^{99m}Tc-CN5DG at 2 min post-injection was 12.97 ± 0.88%ID/g while the uptake value was 0.33 ± 0.06%ID/g at 60 min post-injection. These data suggested that ^{99m}Tc-CN5DG had a fast clearance rate in blood *in vivo*. Major pharmacokinetics parameters are listed in Table 1. The blood distribution half-life was 5.81 min and the blood elimination half-life was 21.16 min.

Abnormal toxicity studies

In the abnormal toxicity study, none of five mice showed abnormality or died after 48 h. If one takes a person weighing 60 kg, the dose received by a mouse (20 g) was about 300 times as much as a human received per kilogram, suggesting the low toxicity of the solution of ^{99m}Tc-CN5DG.
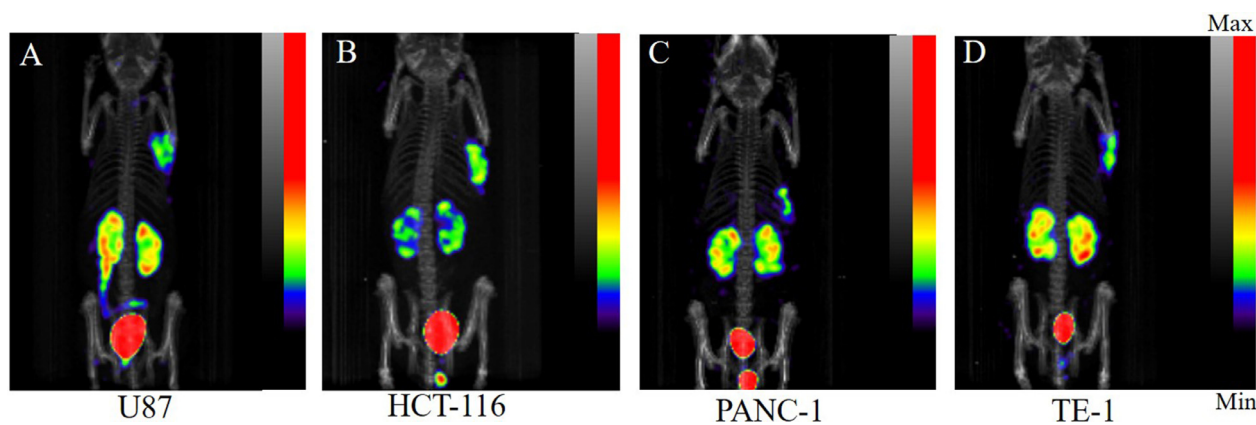
Fig. 3. SPECT/CT images of ^{99m}Tc-CN5DG in nude mice bearing U87 MG(A), HCT-116(B), PANC-1(C) and TE-1(D) tumor xenografts at 2 h after intravenous injection.
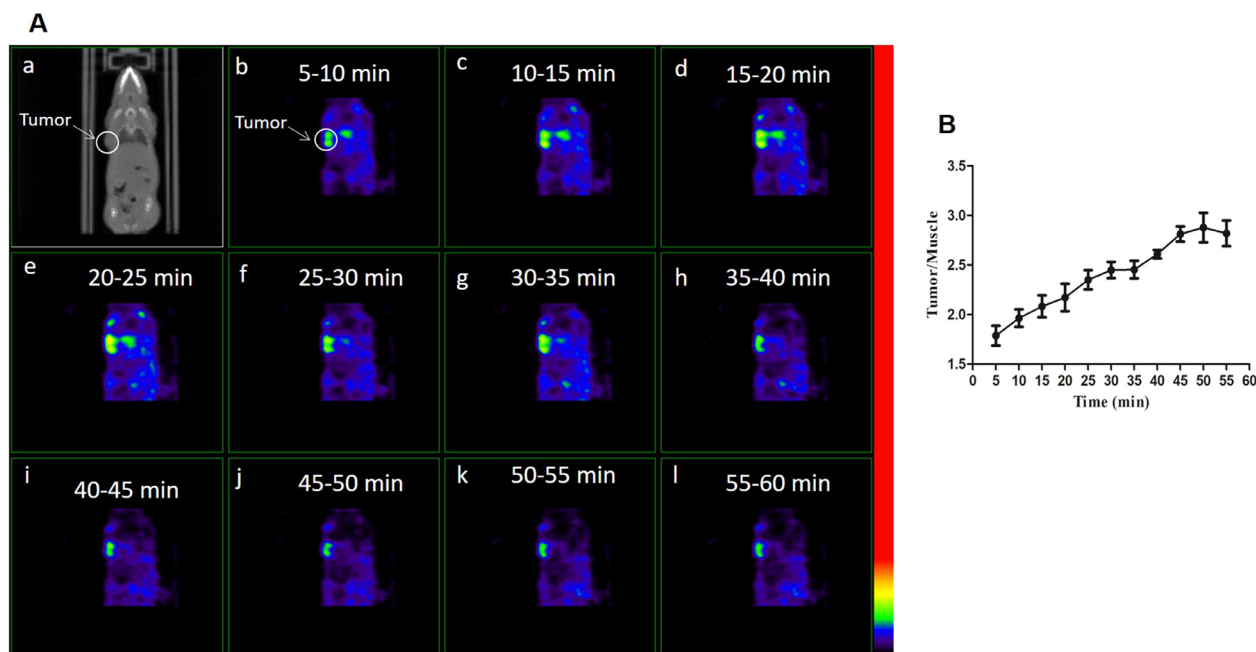

Fig. 4. (A) The dynamic SPECT images of ^{99m}Tc-CN5DG on nude mice bearing U87 MG tumors from 5 min to 60 min post-injection (a, CT; b-l, SPECT). (B) The ROI ratios of tumor/muscle drawn on the SPECT images (b-l).
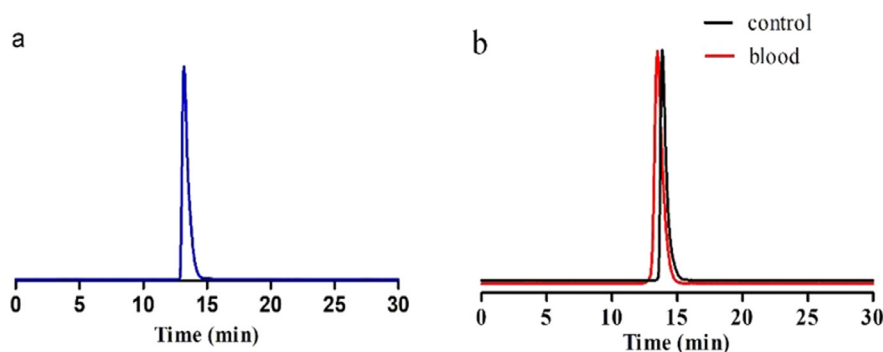

Fig. 5. HPLC profiles of the radioactivity in tumor (a) and blood (b) at 30 min after the injection of ^{99m}Tc-CN5DG in A549 tumor bearing mice.

Discussion

Developing a ^{99m}Tc labeled glucose derivative for tumor detection has been of great importance. In our previous studies, ^{99m}Tc-CN5DG was evaluated in nude mice bearing A549 tumor and would be a potential agent for tumor imaging. In this study, we explored its application in U87 MG, HCT-116, PANC-1 and TE-1 tumor models and its pharmacokinetic characterization *in vivo*.

^{99m}Tc-CN5DG could be readily prepared by using a CN5DG kit (**Fig. 1**). When the pH value of the kit was adjusted to about 6.0, the RCP of the product was more than 95%. Lower pH value (pH < 4.0) is not suitable because isonitrile is not stable under highly acidic conditions. Sodium citrate is a necessary compound in the CN5DG kit to stabi-
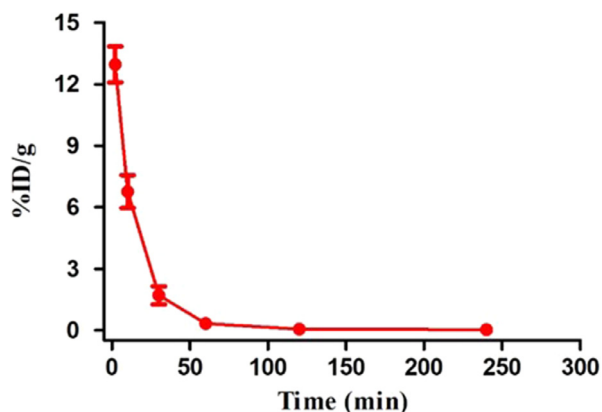
Fig. 6. Time-activity curve of ^{99m}Tc-CN5DG in the blood of healthy mice. Data are expressed as mean ± SD.

Table 1

Major pharmacokinetics parameters derived by two-compartmental modeling after the administration of ^{99m}Tc-CN5DG in healthy CD-1 mice within 4 h post-injection ($n = 6$).

Parameter	Unit	Value
AUC(0-t)	%ID/g $*$min	236.313
AUC(0-∞)	%ID/g $*$min	261.388
t1/2α	min	5.81
t1/2β	min	21.16
V1	L/kg	0.007
V2	L/kg	0.003

lize Sn^{2+} and $^{99m}TcO_2 \bullet nH_2O$ would be formed without it. Commonly, 740 MBq~1110 MBq of ^{99m}Tc labeled radiopharmaceuticals would be used to perform a SPECT scan in clinic, so we studied the radioactivity amount of $^{99m}TcO_4^-$ to prepare ^{99m}Tc-CN5DG. As a result, when the radioactivity of $^{99m}TcO_4^-$ was up to 3700 MBq, the RCP of ^{99m}Tc-CN5DG was still over 95%.

In our previous biodistribution studies in A549 tumor bearing mice, ^{99m}Tc-CN5DG had the highest uptake in tumors at 30 min post-injection and the tumor/muscle ratio was high at 60 min post-injection, but the uptakes in blood and other tissues (such as heart, stomach) were also high at 60 min. It should be noted that the tumor/muscle and tumor/blood ratios were both high at 2 h post-injection. Based on these data, in this study, we performed the biodistribution and SPECT imaging studies at 2 h post-injection to get ideal tumor/non-target ratios. The biodistribution data in four tumor models revealed that ^{99m}Tc-CN5DG had a moderate tumor uptake (from 0.42 ± 0.07%ID/g to 1.24 ± 0.28%ID/g) and high tumor/muscle (from 4.08 ± 0.42 to 9.63 ± 3.53), tumor/blood ratios (from 17.18 ± 7.40 to 53.17 ± 16.16). These data were in accordance with that in A549 tumor model (tumor uptake, 1.48 ± 0.23%ID/g; tumor/muscle ratio, 29.68 ± 3.12; tumor/blood ratio, 60.79 ± 2.86) [24]. The uptake of ^{99m}Tc-CN5DG in U87 MG tumor was significantly lower than that in other three kinds of tumors, possibly because the amounts of Gluts that transport the tracer into U87 MG tumor cells are lower than those on the other three tumor cell lines. This needs further investigation.

The SPECT/CT images of ^{99m}Tc-CN5DG verified its broad-spectrum application in U87 MG, HCT-116, PANC-1 and TE-1 tumor models. The ROIs (regions of interest drawn from SPECT images) ratios of the tumor sites *versus* corresponding non-tumor sites for U87 MG, HCT-116, PANC-1 and TE-1 were 3.09 ± 0.19, 4.73 ± 0.15, 5.51 ± 0.79 and 6.01 ± 1.37, respectively. These data nearly consisted with the tumor/muscle ratios (from 4.08 ± 0.42 to 9.63 ± 3.53) from biodistribution data. Moreover, there is no observable background uptake on SPECT images, suggesting the low uptake in blood, which is also consistence with the

biodistribution data (tumor/blood ratios varied from 17.18 ± 7.40 to 53.17 ± 16.16). In addition, the kidney/tumor ratios in TE-1 and PANC-1 tumor bearing mice are 1.97 and 1.67 from the biodistribution data, while the ROIs ratios of kidney/tumor from SPECT images in TE-1 and PANC-1 are 2.01 and 1.64. The biodistribution data also corresponded with the data drawn on SPECT images. Although U87 MG tumor uptake (0.42 ± 0.07%ID/g) was lower than the uptake in HCT-116, PANC-1 and TE-1 tumors (from 0.95 ± 0.09%ID/g to 1.24 ± 0.28%ID/g), the U87 MG tumor could also be clearly seen in the whole-body SPECT/CT images. Dynamic SPECT images further verified that the U87 MG tumors could be detected at 5 min after the injection of ^{99m}Tc-CN5DG. These results warranted the early tumor detection ability of ^{99m}Tc-CN5DG in other three kinds of tumor models (HCT-116, PANC-1 and TE-1). When compared to $[^{18}F]$FDG, ^{99m}Tc-CN5DG has very low physiological uptake in the brain (0.02%ID/g). As presented in Fig. 1, ^{99m}Tc-CN5DG is a positively charged complex, while $[^{18}F]$FDG is a neutral molecule. Hence, $[^{18}F]$FDG can cross the blood-brain barrier easily while ^{99m}Tc-CN5DG can't. So little uptake of ^{99m}Tc-CN5DG was observed in mouse brain. As a result, the tumor/brain ratio of ^{99m}Tc-CN5DG in U87 MG tumor bearing mice was high (19.00 ± 0.71). This findings may compensate the deficiency of $[^{18}F]$FDG for brain tumor detection.

The evaluation of ^{99m}Tc-CN5DG as a tumor imaging agent was initially studied in A549 tumor bearing nude mice (including tumor uptake studies, biodistribution studies, SPECT/CT imaging studies) [24], as a continuous study of this work, A549 tumor bearing mice were used for the metabolic study of ^{99m}Tc-CN5DG *in vivo*. In this study, ^{99m}Tc-CN5DG was also found to be stable in blood and had no other metabolite in A549 tumors, suggesting it exhibited high stability *in vivo*. The significant tumor uptake, fast blood clearance and good safety of ^{99m}Tc-CN5DG warranted its further clinical application for cancer diagnosis.

Conclusion

In this study, ^{99m}Tc-CN5DG exhibited moderate tumor uptake, tumor/muscle and tumor/blood ratios in U87 MG, HCT-116, PANC-1 and TE-1 tumor models. SPECT/CT images in four tumor models demonstrated that all four kinds of tumors could be clearly detected. Moreover, ^{99m}Tc-CN5DG was stable in blood and tumors *in vivo* and rapidly cleared from blood. These findings verified ^{99m}Tc-CN5DG could be used as a promising broad-spectrum tumor imaging agent and had potential for clinical translation.

Declaration of Competing Interest

The authors declare that they have no known competing financial interests or personal relationships that could have appeared to influence the work reported in this paper.

CRediT authorship contribution statement

Xuran Zhang: Conceptualization, Methodology, Validation, Investigation, Writing - original draft. **Qing Ruan:** Investigation, Validation. **Yuhao Jiang:** Investigation, Validation. **Qianqian Gan:** Investigation, Validation. **Junbo Zhang:** Conceptualization, Validation, Resources, Writing - review & editing, Supervision.

Funding

References

[1] P. Brugarolas, J. Comstock, D.W. Dick, T. Ellmer, J.W. Engle, S.E. Lapi, S.H. Liang, E.E. Parent, P.N.V. Kishore, S. Selivanova, et al., Fifty years of radiopharmaceuticals, J. Nucl. Med. Technol. 48 (Suppl 1) (2020) 34S–39S.

[2] J.K. Willmann, N. van Bruggen, L.M. Dinkelborg, S.S. Gambhir, Molecular imaging in drug development, Nat. Rev. Drug. Discov. 7 (7) (2008) 591–607.

[3] A. Niyonkuru, X. Chen, K.H. Bakari, D.N. Wimalarathne, A. Bouhari, M.M.R. Arnous, X. Lan, Evaluation of the diagnostic efficacy of ^{18}F-fluorine-2-deoxy-D-glucose PET/CT for lung cancer and pulmonary tuberculosis in a tuberculosis-endemic country, Cancer Med. 9 (3) (2020) 931–942.

[4] E. Acar, B. Turgut, S. Yigit, G. Kaya, Comparison of the volumetric and radiomics findings of ^{18}F-FDG PET/CT images with immunohistochemical prognostic factors in local/locally advanced breast cancer, Nucl. Med. Commun. 40 (7) (2019) 764–772.

[5] A. Collarino, G. Garganese, R.A.V. Olmos, A. Stefanelli, G. Perotti, P. Mirk, S.M. Fragomeni, F.P. Ieria, G. Scambia, A. Giordano, et al., Evaluation of dual-time-point ^{18}F-FDG PET/CT imaging for lymph node staging in vulvar cancer, J. Nucl. Med. 58 (12) (2017) 1913–1919.

[6] K. Sasaki, Y. Uchikado, H. Okumura, I. Omoto, Y. Kita, T. Arigami, Y. Uenosono, T. Owaki, K. Maemura, S. Natsugoe, Role of ^{18}F-FDG-PET/CT in esophageal squamous cell carcinoma after neoadjuvant chemoradiotherapy, Anticancer Res. 37 (2) (2017) 859–864.

[7] J.W. Lee, C.M. Kang, H.J. Choi, W.J. Lee, S.Y. Song, J.-.H. Lee, J.D. Lee, Prognostic value of metabolic tumor volume and total lesion glycolysis on preoperative ^{18}F-FDG PET/CT in patients with pancreatic cancer, J. Nucl. Med. 55 (6) (2014) 898–904.

[8] X. Chen, L. Li, F. Liu, B. Liu, Synthesis and biological evaluation of technetium-99m-labeled deoxyglucose derivatives as imaging agents for tumor, Bioorg. Med. Chem. Lett. 16 (21) (2006) 5503–5506.

[9] J. Liang, Y. Chen, Z. Huang, Y. Zhao, L. He, Early chemotherapy response evaluation in tumors by ^{99m}Tc-DTPA-DG, Cancer Biother. Radiopharm. 23 (3) (2008) 363–370.

[10] A.L. Branco de Barros, V.N. Cardoso, LdG Mota, E.A. Leite, M.C. de Oliveira, R.J. Alves, Synthesis and biological evaluation of technetium-labeled -glucose-MAG$_3$ derivative as agent for tumor diagnosis, Bioorg. Med. Chem. Lett. 19 (9) (2009) 2497–2499.

[11] R. Dapueto, R. Castelli, M. Fernandez, J.A. Chabalgoity, M. Moreno, J.P. Gambini, P. Cabral, W. Porcal, Biological evaluation of glucose and deoxyglucose derivatives radiolabeled with [[99m]Tc(CO)$_3$(H$_2$O)$_3$]$^+$ core as potential melanoma imaging agents, Bioorg. Med. Chem. Lett. 21 (23) (2011) 7102–7106.

[12] S.J. Oh, J.-.S. Ryu, E.-.J. Yoon, M.S. Bae, S.J. Choi, K.B. Park, D.H. Moon, ^{99m}Tc-labeled 1-thio-β-D-glucose as a new tumor-seeking agent: synthesis and tumor cell uptake assay, Appl. Radiat. Isot. 64 (2) (2006) 207–215.

[13] J. Ding, H. Su, F. Wang, T. Chu, A pre-targeting strategy for imaging glucose metabolism using technetium-99m labelled dibenzocyclooctyne derivative, Bioorg. Med. Chem. Lett. 29 (14) (2019) 1791–1798.

[14] S. Singh, S. Singh, R.K. Sharma, A. Kaul, R. Mathur, S. Tomar, R. Varshney, A.K. Mishra, Synthesis and preliminary evaluation of a ^{99m}Tc labelled deoxyglucose complex {[^{99m}Tc]DTPA-bis(DG)} as a potential SPECT based probe for tumor imaging, New J. Chem. 44 (7) (2020) 3062–3071.

[15] D.J. Yang, C.-.G. Kim, N.R. Schechter, A. Azhdarinia, D.-F Yu, C.-.S. Oh, J.L. Bryant, J.-.J. Won, E.E. Kim, D.A. Podoloff, Imaging with ^{99m}Tc ECDG targeted at the multifunctional glucose transport system: feasibility study with rodents, Radiology 226 (2) (2003) 465–473.

[16] N.R. Schechter, W.D. Erwin, D.J. Yang, E.E. Kim, R.F. Munden, K. Forster, L.C. Taing, J.D. Cox, H.A. Macapinlac, D.A. Podoloff, Radiation dosimetry and biodistribution of ^{99m}Tc-ethylene dicysteine-deoxyglucose in patients with non-small-cell lung cancer, Eur. J. Nucl. Med. Mol. Imaging 36 (10) (2009) 1583–1591.

[17] T. Liu, J. Zhang, X. Wang, J. Yang, Z. Tang, J. Lu, Radiolabeled glucose derivatives for tumor imaging using SPECT and PET, Curr. Med. Chem. 21 (1) (2014) 24–34.

[18] T. Liu, Q. Gan, J. Zhang, Z. Jin, W. Zhang, Y. Zhang, Synthesis and biodistribution of novel [99m]TcN complexes of glucose dithiocarbamate as potential probes for tumor imaging, Medchemcomm 7 (7) (2016) 1381–1386.

[19] T. Liu, Q. Gan, J. Zhang, Macrocyclic triamine derived glucose analogues for [99m]Tc(CO)$_3$ labeling: synthesis and biological evaluation as potential tumor-imaging agents, Chem. Biol. Drug Des. 89 (2) (2017) 277–284.

[20] X. Lin, Z. Jin, J. Ren, Y. Pang, W. Zhang, J. Huo, X. Wang, J. Zhang, Y. Zhang, Synthesis and biodistribution of a new ^{99m}Tc-oxo complex with deoxyglucose dithiocarbamate for tumor imaging, Chem. Biol. Drug Des. 79 (3) (2012) 239–245.

[21] J. Zhang, J. Ren, X. Lin, X. Wang, Synthesis and biological evaluation of a novel ^{99m}Tc nitrido radiopharmaceutical with deoxyglucose dithiocarbamate, showing tumor uptake, Bioorg. Med. Chem. Lett. 19 (10) (2009) 2752–2754.

[22] Y. Wang, J. Zhu, X. Song, X. Wang, J. Yang, J. Zhang, Synthesis and evaluation of ^{99m}Tc-2-[(3-carboxy-1-oxopropyl)amino]-2-deoxy-D-glucose as a potential tumor imaging agent, Bioorg. Med. Chem. Lett. 24 (16) (2014) 3882–3885.

[23] X. Zhang, Q. Gan, Q. Ruan, D. Xiao, J. Zhang, Evaluation and comparison of ^{99m}Tc-labeled D-glucosamine derivatives with different ^{99m}Tc cores as potential tumor imaging agents, Appl. Organomet. Chem. (2020), doi:10.1002/aoc.6008.

[24] X. Zhang, Q. Ruan, X. Duan, Q. Gan, X. Song, S. Fang, X. Lin, J. Du, J. Zhang, Novel ^{99m}Tc-labeled glucose derivative for single photon emission computed tomography: a promising tumor imaging agent, Mol. Pharm. 15 (8) (2018) 3417–3424.

[25] J. Li, C. Peng, Z. Guo, C. Shi, R. Zhuang, X. Hong, X. Wang, D. Xu, P. Zhang, D. Zhang, et al., Radioiodinated pentixather for SPECT imaging of expression of the chemokine receptor CXCR4 in rat myocardial-infarction-reperfusion models, Anal. Chem. 90 (15) (2018) 9614–9620.